Seismic Performance Enhancement of Base-Isolation Using Semi-Active Damping Devices

Yunbyeong Chae and James M. Ricles
Department of Civil and Environmental Engineering, Lehigh University, USA

SUMMARY:
The use of semi-active devices can be a viable solution to decrease the acceleration demand in base-isolated structures under short-period ground motions while it can maximize the damping force under long-period ground motions by adaptively activating/deactivating the damper according to a control law based on structural response. A robust new semi-active controller is developed based on acceleration feedback and the transmissibility of the base-isolation system. This semi-active controller not only effectively reduces the resonance effect of a base-isolation system that can occur under long-period ground motions, but also reduces the base isolator bearing displacement demand and base shear under short-period ground motions. The statistical results from a series of numerical simulations are provided and discussed to validate the performance improvement and robustness of the newly developed semi-active controller.

Keywords: base isolation, semi-active control, vibration reduction

1. INTRODUCTION

Base Isolation is one of the more widely implemented and accepted seismic protection systems used in practice. Seismic base isolation (Skinner et al. 1993; Naeim and Kelly 1999) is a technique that mitigates the effects of an earthquake by essentially isolating the structure and its contents from potentially dangerous ground motions, especially in the frequency range where the building is most affected. The goal is to simultaneously reduce interstory drift and floor accelerations in order to limit or avoid damage, not only to the structure but also to its contents, in a cost-effective manner.

In the late 1970s through the early 90's there were several significant structural failures due to severe seismic events (e.g., 1979 Imperial Valley EQ, 1989 Loma Prieta EQ, 1994 Northridge EQ, 1995 Kobe EQ) that have had a major influence on current code requirements for base isolation design. Based on observations from the January 17, 1994 Northridge earthquake, it was suggested (Hall et al. 1995 and Heaton et al. 1995) that base-isolated buildings are vulnerable to strong impulsive ground motions generated at near-source locations. Near-fault ground motions often have pulses in the accelerogram that lead to large ground velocities, resulting in long-period ground motion characteristics. Conventional base-isolation systems perform well under strong short-period ground motions by elongating the fundamental period of the structure. Under long-period ground motions significant spectral accelerations occur at the longer periods, which amplify the response at the longer periods of vibration which can lead to a resonance effect in a conventional base-isolation system.

Several near-fault ground motions recorded in Southern California clearly show strong long-period content with spectral accelerations that are higher than the maximum considered earthquake (MCE) level used in current codes. The MCE ground motion is represented by a response spectra that has a 2% probability of exceedance in 50 years, and the design basis earthquake (DBE) ground motion is $2/3^{rd}$ the intensity of the MCE ground motion. (FEMA 2003). Response spectra of recent Southern California (Imperial Valley: Mw 6.53; Northridge: Mw 6.69) and Northern California (Loma Prieta: Mw 6.93)

earthquakes where the rupture distances is less than 10 km from the recorder are given in Figure 1.1. Included in Figure 1.1 are the site specific response spectra for the DBE and MCE for van Nuys, Los Angeles (ASCE 2010) In Figure 1.1 it is apparent that the response spectra of these earthquakes exceed the MCE response spectrum at longer periods.

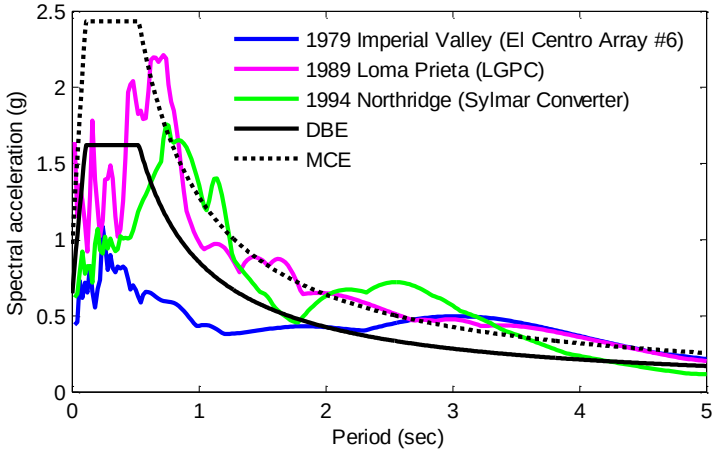

Figure 1.1. Response spectra of recent California earthquakes

In order to improve the performance of base isolation systems under strong near-fault ground motions, an innovative method is developed that utilizes semi-active damping devices. The method is based on the transmissibility of base-isolation systems. A semi-active damping device is used to adequately reduce the transmitted force to the superstructure, thereby reducing the story drifts and floor accelerations developed in the superstructure. A new semi-active control algorithm based on the transmissibility is presented and a series of numerical simulations are conducted to assess the performance of this new algorithm.

2. BASE ISOLATION WITH SEMI-ACTIVE DEVICES

During the last decade, numerous studies on semi-active control algorithms applied to base-isolation systems combined with semi-active devices have been conducted to improve the performance of the conventional base-isolation systems. Semi-active devices can offer the adaptability of active control devices without requiring the associated large power sources (Spencer and Sain 1997), which is important during large earthquakes when a power blackout may occur. These studies focused on adding controlled supplemental damping to achieve low interstory drift while limiting the maximum isolator bearing displacement with a single set of control forces. The studies include numerical simulations that employed semi-active viscous dampers (Nagarajaiah 1994; Symans and Kelly 1999; and Madden et al. 2002), electrorheological dampers (Makris 1997), magnetorhelogical dampers (Johnson et al. 1998, 1999 and Ramallo et al. 2000), tuned interaction dampers (Zhang and Iwan 2002) and semi-active stiffness dampers (Agrawal and Yang 2000). Experimental studies have been performed which employed semi-active friction dampers (Fujita et al. 1994), semi-active viscous dampers (Symans et al. 2000), magnetorheological dampers (Nagarajaiah et al. 2000, Yoshioka et al. 2002, Tu et al. 2010) and adaptive sliding isolators (Madden et al. 2002). A majority of the experimental studies involved reduced scale models.

In spite of these efforts, however, most of existing studies on base isolation systems with semi-active devices resulted in only a marginal performance improvement compared to the passive base isolation systems (Reigles and Symans 2005). This may be attributed to the fact that the control laws for the semi-active devices are often based on control objectives that are not directly related to minimizing the maximum structural responses of interest, (e.g., the isolator displacement, story drifts, floor accelerations). For example, in the design of Linear Quadratic Gaussian (LQG) algorithms (Ramallo et al. 2002; Yoshioka et al. 2002) and Sliding Mode Control (SMC) (Madden et al. 2002; Tsuchimoto et al.

2005; Fan et al. 2009) the control objective is based on minimizing a quadratic cost function over the entire duration of the earthquake (Ogata 1997). Chae (2011) showed that minimizing the quadratic cost function does not always lead to the minimization of the maximum structural response. Moreover, finding the optimal user-defined parameters (i.e., weights) for these controllers is a challenging task, making it difficult to be widely used in practice.

There are other semi-active controllers utilizing neural networks (Lee et al. 2005; Bani-Hani and Sheban 2006) and fuzzy controllers (Wongprasert and Symans 2005; Reigles and Symans 2006; Lin et al. 2007), which are based on a special nonlinear system that correlates the input (e.g., feedback response) and output data (e.g., command signal to semi-active devices). The optimization of the nonlinear system depends on the training set (neural networks) and fuzzy logics tuned from selected ground motions (fuzzy controls). Thus, the performance of these controllers depends on the selection of pre-defined data set, implying the nonlinear system may not work well for other inputs which have different characteristics from the pre-defined data set.

Semi-active devices are still attractive since they can adaptively control the force of device to the response of a structure. However, a robust semi-active control algorithm needs to be developed which can improve the performance significantly over the passive system so that the additional cost associated with operating semi-actively controlled base isolation system can be justified.

3. NEWLY DEVELOPED SEMI-ACTIVE CONTROL ALGORITHM

A new semi-active control algorithm is developed to achieve a better resiliency than a passive base isolation system. The new algorithm is based on reducing the transmitted force to the superstructure by adaptively adjusting the damping of a base isolator. Controlling the damping over a wide frequency range to reduce the transmissibility of forces and accelerations across the interface of the isolation system forms the basic concept of the new algorithm, where an isolation system with a semi active device controlled by this algorithm is referred to herein as the *Controlled-Damping Isolation* (CDI) System.

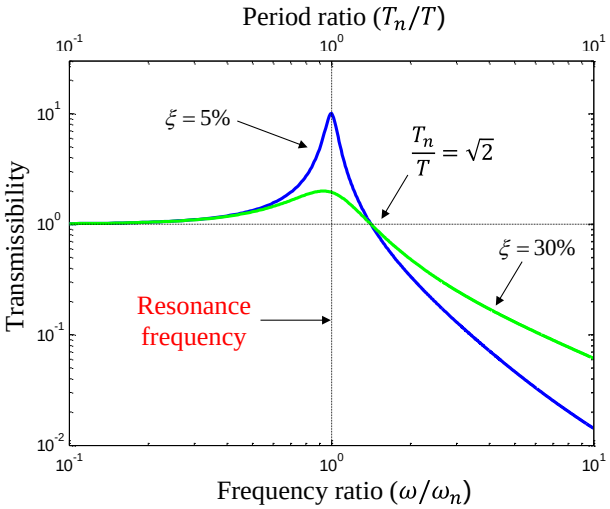

Figure 3.1. Transmissibility of harmonic excitation of SDOF system

Figure 3.1 shows the transmissibility of force and accelerations for an SDOF system for the cases of low damping (ξ=5%) and high damping (ξ=30%). The transmitted force to the superstructure is maximum when the excitation frequency (ω) approaches the natural frequency of the system (ω_n), (or the excitation period (T) approaches the natural period (T_n)), which is representative of the response of a base-isolated building to a long period, near-fault motion. Figure 3.1 suggests that higher damping is desirable during a long period excitation, while lower damping is desirable during a short period

excitation. Therefore, with controlled damping the force and accelerations transmitted to the superstructure can be minimized by maximizing the damping under low-frequency (long-period), and by minimizing the damping under high-frequency (short-period) excitations. Simultaneously, selectively controlling the damping in the isolation system will also reduce the deformation across the isolation interface.

The CDI system consists of a semi-actively controlled damper placed adjacent to a low damping rubber isolation bearing that develops the same deformations as the bearing. Assuming that a base-isolated system is predominantly governed by the fundamental mode, the transmitted force to the superstructure is closely related to its base floor acceleration $a(t)_{base}$. Based on this assumption, the following control law is considered, where the damper force f_d supplied by the semi-active damping device is:

$$f_d = \begin{cases} f_{d\_max}; & \text{if } T_{cross} \geq \gamma_T T_{iso}, \text{ or } |a(t)_{base}| < a_{pr} \\ f_{d\_min}; & \text{otherwise} \end{cases} \tag{3.1}$$

In Equation (3.1) f_{d_max} and f_{d_min} are the maximum and minimum force that can be achieved in the damper (e.g., in the case of MR dampers when the current is turned on and off, respectively). T_{iso} is the fundamental period of the isolated structure, $0.5 * T_{cross}$ is the time between zero-crossings of the $a(t)_{base}$, and γ_T is a constant. T_{cross} is based on the measured feedback signal for $a(t)_{base}$ and the detection of zero crossing. Simple methods to detect zero crossings are given by Wall (2003). The value for γ_T can be established by considering the transmissibility plot in Figure 3.1, where if $T_{iso}/\sqrt{2} < T_{cross}$ then the resonance condition is potentially being approached and the damper is operated to produce its maximum damper force. To ensure a reduction in the isolator deformation, the CDI also activates the semi-active damping device under a moderate acceleration response. Therefore, when $|a(t)_{base}|$ is less than a pre-defined level of acceleration, a_{pr}, the semi-active damper is activated (e.g., maximum current for an MR damper is used) to reduce the isolator deformation by dissipating more energy in the base-isolation system. In this study, values of γ_T =1/√2 and a_{pr}=0.1g were used in the control law. Unlike most existing semi-active control algorithms for base-isolation systems, which require full-feedback data, the CDI only needs the acceleration feedback of the base floor level, $a(t)_{base}$.

4. NUMERICAL SIMULATIONS

4.1. Prototype Structure

The performance of the CDI system is evaluated by comparing its ability to reduce structural response with a conventional passive base isolation system. The 3-story building structure shown in Figure 4.1 is used as the superstructure. The building is located in the Los Angeles area and constructed with a steel MRF as the lateral load resisting system. The building is modeled as a linear shear building structure where the mass and story stiffness are given as: $m_b = m_1 = m_2 = m_3 = 400\text{kN} \cdot \sec^2/\text{m}$, $k_1 = 41{,}895\text{kN/m}$, $k_2 = 32{,}227\text{kN/m}$, and $k_3 = 22{,}559\text{kN/m}$. The passive base isolator of this study (see Figure 4.1(b)) is modeled using the Kelvin-Voigt element where the linear spring and dashpot are combined together in parallel. The effective stiffness of the base isolator, k_b, is calculated in accordance with ASCE7-10 (ASCE 2010), where

$$k_b = \frac{4\pi^2 W}{T_{eff}^2 g} \tag{4.1}$$

In Equation (4.1) W is the effective seismic weight of the structure above the isolation interface and g is the acceleration due to gravity. The target effective period of the isolated building is equal to T_{eff}=3.0sec.

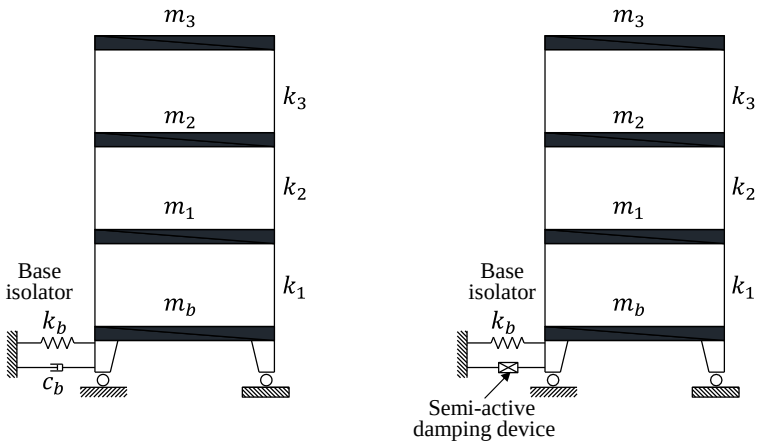

(a)

(b)

Figure 4.1. 3-story building structure with base isolation system: (a) passive base isolation; (b) semi-active base isolation

Thus, the effective stiffness of the base isolator calculated from Equation (4.1) is $k_b = 7{,}018\text{kN/m}$. The damping coefficient of the base isolator is expressed as:

$$c_b = 2\xi_{eff}\frac{W}{g}\frac{2\pi}{T_{eff}} \tag{4.2}$$

where, ξ_{eff} is the effective damping ratio. Four design cases were considered in this study: (1) passive base-isolation with an isolator equivalent damping ratio of ξ_{eff} = 8% of critical; (2) passive base-isolation with ξ_{eff}=15% of critical; (3) passive base-isolation with ξ_{eff}=30% of critical; and (4) smart base isolation system that incorporates the CDI concept. The low damping case of ξ_{eff} is achieved through a natural rubber bearing, while the moderate and high damping cases can generally be achieved by using lead-rubber bearings. For the case with the CDI system, a variable orifice damper which can modify the damping coefficient according to a command signal is used. The variable orifice damper is assumed to be able to vary the effective damping ratio from 8% to 30%, resulting in c_b^{min}= 536kN-sec/m and c_b^{max} = 2011kN-sec/m for the minimum and maximum damping coefficients, respectively. The dynamics of the variable orifice damper associated with the control of the valve that controls the flow is assumed to be governed by a first order filter,

$$\frac{dc_{var}}{dt} = \eta(c_{com} - c_{var}) \tag{4.3}$$

where c_{var} is a damping coefficient of the variable orifice damper and c_{com} is the command damping coefficient which is either c_b^{min} or c_b^{max}. η is a filter coefficient. In this study, η=6 is used to model the dynamics of the variable orifice damper, where this value results in about a 0.5sec rise time to reach the 95% of targeted damping coefficient.

The story stiffness of the base-isolated building is selected to satisfy the code maximum story drift limit of 1.5% under the DBE in accordance with ASCE7-10 (ASCE 2010). The fundamental period of the isolated building and the superstructure without base isolation are provided in Table 4.1.

Table 4.1. Fundamental natural periods of building

	Natural periods (sec)		
	T_1	T_2	T_3
Superstructure only	1.51	0.60	0.40
Isolated building	3.26	0.89	0.51

4.2. Ground Motions

In order to compare the performance of the four isolation cases, time history analyses are performed using an ensemble of ground motions to obtain the statistical response. The LA-SAC suite of ground motions (Sommerville et al. 1997) was selected as the ground motions. The comparisons involve two different hazard levels: records with a 10% in 50 year probability of exceedance, (i.e. the design basis earthquake (DBE)); and records with a 2% in 50 year probability of exceedance (maximum considered earthquake (MCE)). Figure 4.2 shows the response spectra of the LA-SAC ground motions for a damping ratio of 5%.

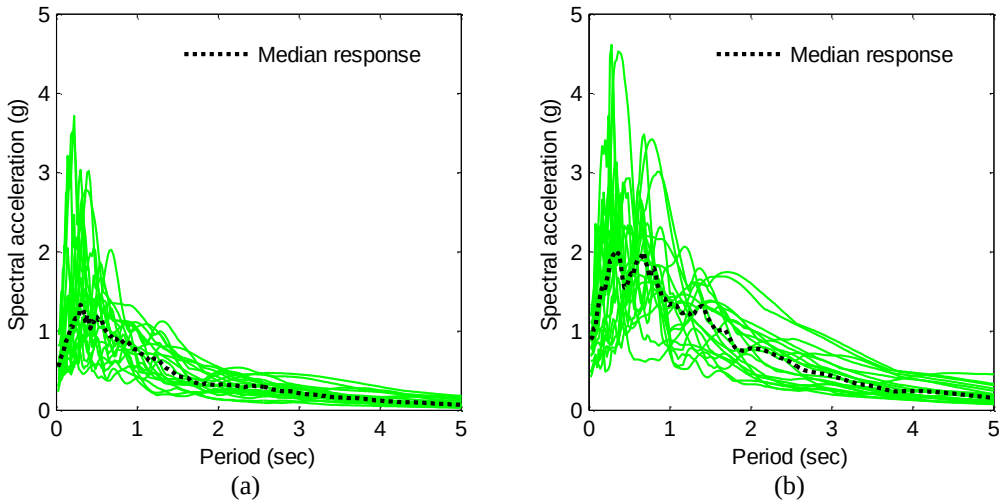

Figure 4.2. Response spectra of LA-SAC ground motions: (a) DBE level; (b) MCE level

4.3. Numerical Simulation Results

The median values of the maximum response to an ensemble of LA-SAC ground motions are given in Tables 4.2 through 4.5. The results in Table 4.2 compare the median maximum isolator bearing deformation, δ_{br}, and the ratio of maximum base shear to the weight of the building, (Vb_{max}/W). The design base shear and the maximum deformation of the isolator bearing are determined from the response under the DBE and MCE, respectively (ASCE 2010). It is clear that increasing damping in the isolator system is beneficial towards reducing the isolator bearing maximum deformation and maximum base shear. By using a high damping (ξ_{eff}=30%) isolator, the maximum isolator bearing deformation is reduced by about 26% under the MCE compared to the low damping isolator (ξ_{eff}=8%). The CDI system results in about the same performance as the high damping isolator in reducing the isolator deformation. However, the CDI results in the minimum base shear under the DBE, which is closely related to the design of the superstructure. The maximum base shear with the CDI is reduced by about 17%, 11%, and 11% compared to the low damping, moderate damping (ξ_{eff}=15%), and high damping cases, respectively. Reduced base shear is economical whereby it enables a reduction in the design base shear and the cost of superstructure.

Table 4.2. Median maximum isolator bearing deformation (δ_{br}) and ratio of maximum base shear (Vb_{max}) to weight of building (W)

Hazard level	δ_{br} (m)				Vb_{max}/W			
	ξ_{eff}=8%	ξ_{eff}=15%	ξ_{eff}=30%	CDI	ξ_{eff}=8%	ξ_{eff}=15%	ξ_{eff}=30%	CDI
DBE	0.322	0.287	0.230	0.248	0.150	0.141	0.140	0.125
MCE	0.630	0.584	0.468	0.491	0.291	0.283	0.282	0.265

There is a well-known trade-off between the isolator deformation and the response of superstructure in

the passive base isolation system (Chopra 1996, Morgan and Mahin 2010). The reduced isolation deformation is achieved by increasing the damping of the base isolator, but the increase in maximum story drift and absolute accelerations are observed as summarized in Tables 4.3 and 4.4. Under the MCE, for example, the 3rd story drift and 3rd floor acceleration are increased by 5% and 7%, respectively, when the damping is increased from ξ_{eff} =8% to ξ_{eff} =30%, while the isolator deformation is reduced by 26%. The CDI system, however, does not increase the response of the superstructure like the high damping passive isolator. It shows overall an improved performance compared to the passive base isolation systems throughout the story drift, velocity, and acceleration. Under the MCE the CDI results in about the same isolator bearing deformation as the high damping case, with a reduction in maximum 2nd story drift and 3rd floor acceleration of about 15% and 20%, respectively, demonstrating a superior performance of the CDI system. Compared to the low damping case, the maximum velocity at the 3rd floor is reduced by about 13% under the MCE (Table 4.5). The absolute velocity and acceleration are directly related to the response and damage of nonstructural components. Since the CDI is based on the reduction of the transmitted force to the superstructure under the wide range of frequencies of earthquake ground motions, it can effectively reduce both the isolation deformation and the response of the superstructure.

Table 4.3. Median maximum story drift (%)

Story	DBE				MCE			
	ξ_{eff}=8%	ξ_{eff}=15%	ξ_{eff}=30%	CDI	ξ_{eff}=8%	ξ_{eff}=15%	ξ_{eff}=30%	CDI
1	1.26	1.20	1.25	1.18	2.45	2.37	2.32	2.16
2	1.29	1.27	1.33	1.24	2.58	2.51	2.72	2.36
3	1.17	1.14	1.22	1.16	2.35	2.35	2.47	2.11

Table 4.4 Median maximum absolute floor acceleration (g)

Floor level	DBE				MCE			
	ξ_{eff}=8%	ξ_{eff}=15%	ξ_{eff}=30%	CDI	ξ_{eff}=8%	ξ_{eff}=15%	ξ_{eff}=30%	CDI
Base	0.194	0.198	0.244	0.205	0.349	0.372	0.423	0.346
1	0.190	0.198	0.219	0.195	0.344	0.354	0.377	0.331
2	0.184	0.182	0.215	0.190	0.387	0.373	0.393	0.349
3	0.246	0.247	0.266	0.255	0.509	0.505	0.546	0.457

Table 4.5. Median maximum absolute floor velocity (m/sec)

Floor level	DBE				MCE			
	ξ_{eff}=8%	ξ_{eff}=15%	ξ_{eff}=30%	CDI	ξ_{eff}=8%	ξ_{eff}=15%	ξ_{eff}=30%	CDI
Base	0.63	0.54	0.52	0.52	1.13	1.02	0.93	1.04
1	0.69	0.63	0.59	0.60	1.19	1.04	1.06	1.06
2	0.80	0.73	0.68	0.69	1.44	1.35	1.30	1.26
3	0.94	0.86	0.81	0.79	1.72	1.63	1.62	1.50

5. SUMMARY

Conventional base-isolation systems perform well under strong short-period ground motions by elongating the fundamental period of the structure. However, a conventional base-isolation system under long-period ground motions is not as effective in reducing structural response under short-period ground motions because of the resonance effect. Under long-period ground motions, increasing the damping is beneficial to reduce the resonance effect and the response of the superstructure. The increase

in damping, however, increases the story drift and absolute accelerations of the superstructure, thus defeating many of the gains base isolation is intended to provide.

A new semi-active control algorithm is used to create the *Controlled-Damping Isolation* (CDI) System. The CDI system is proposed to improve the performance of a base-isolated building under a wide range of ground motion periods. The CDI system adaptively controls the damping of the isolator based on the response of building in such a way to reduce the transmitted force to the superstructure. Statistical results from time history analysis for a 3-story building under LA-SAC ground motions were presented to compare the performance of CDI system with a passive base isolation system with various effective damping ratios. The CDI system resulted in about the same isolator bearing deformation as the high damping passive case, while the story drift, velocity, and acceleration demands of the superstructure are less than those of the passive base isolation systems, improving reliability and resiliency of isolated buildings.

The numerical simulations in this study are based on a 3-story building with the assumption of linear-elastic behavior of the structure. Thus, further studies need to be conducted with nonlinear structural models, include more various building configurations, as well as an experimental validation to draw more general conclusion on the performance of CDI system. Moreover, a response prediction method and performance-based design procedure for structures with the CDI system need to be developed for the application of CDI system to civil infrastructure.

REFERENCES

ASCE. (2010). Minimum Design Loads for Buildings and Other Structures, *ASCE Standard ASCE/SEI 7-10*, American Society of Civil Engineers, Reston, VA.

Agrawal, A. K., and Yang, J. N. (2000). A semi-active hybrid isolation system for buildings subjected to near-field earthquakes. *Proc., 14th Conf. on Analysis and Computation held in Conjunction with ASCE Structures Congress 2000*, ASCE, Philadelphia.

Bani-Hani, K.A. and Sheban, M.A. (2006). Semi-active neuro-control for base- isolation system using magnetorheological (MR) dampers. *Earthquake Engng. Struct. Dyn.*, **35**, 1119-1144

Chae, Y. (2011). Seismic hazard mitigation of building structures using magneto-rheological dampers. *Ph.D. Dissertation*, Department of Civil and Environmental Engineering, Lehigh University, Bethlehem, PA.

Chopra, A.K. (1995). Dynamics of structurce: theory and application to earthquake engineering. Prentice hall, New Jersey.

Fan, Y-C., Chin-Hsiung Loh, C-H, Yang, J.N., and Lin, P-Y. (2009) Experimental performance evaluation of an equipment isolation using MR dampers. *Earthquake Engineering and Structural Dynamics*, **38**, 285-305.

Federal Emergency Management Agency. (2003). NHRP recommended provisions for seismic regulations for new buildings and other structures. *Report No. FEMA-450*. Washington, DC.

Fujita et al. (1994) Semiactive seismic isolation system using controllable friction damper. *Bull. ERS*, **27**, 21–31.

Hall J.F., Heaton T.H., Halling, M.W., and Wald D.J. (1995). Near-source ground motion and its effects on flexible buildings. *Earthquake Spectra*, **11:4**, 569-605.

Heaton, T.H., Hall, J.F., Wald, D.J., and Halling, M.V. (1995). Response of high-rise and base-isolated buildings in a hypothetical Mw 7.0 blind thrust earthquake. *Science*, **267**, 206–211.

Johnson, E. A., Ramallo, J. C., Spencer, B. F., and Sain, M. K. (1999) Intelligent base isolation systems. *Proc., 2nd World Conf. on Structural Control*, Kyoto, Japan, June, 367–376.

Johnson, E.A., Ramallo, J., Spencer, Jr., B.F., and Sain, M. K. (1998). Intelligent base isolation systems. *Proc., 2nd World Conf. on Structural Control*, Wiley, New York.

Lee, H.J., Jung, H.J., Yun, W.H., and Lee, I.W. (2005). Semi-actve Neuro-Control using MR Damper for Base-Isolated Benchmark Problem. *The Eighteenth KKCNN Symposimum on Civil Engineering*, Taiwan.

Lin, P.Y., Roschke, P.N., and Loh, C.H. (2007). Hybrid base-isolation with magnetorheological damper and fuzzy control. *Structural Control and Health Monitoring*, **14**, 384-405.

Madden, G. J., Symans, M. D., and Wongprasert, N. (2002). Experimental verification of seismic response of building frame with adaptive sliding base-isolation system. *Journal of Structural Engineering*, **128:8**, 1037–1045.

Makris, N. (1997). Rigidity-plasticity-viscosity: Can electrorheological dampers protect base-isolated structures from near-source earthquakes. *Earthquake Engineering and Structural Dynamics*, **26**, 571–591.

Morgan, T.A. and Mahin S.A. (2010). Achieving reliable seismic performance enhancement using muti-stage

friction pendulum isolators. *Earthquake Engineering and Structural Dyanmics*, **39**, 1443-1461.
Naeim, F., and Kelly, J. M. (1999). Design of seismic isolated structures: From theory to practice, Wiley, Chichester, England
Nagarajaiah, S. (1994). Fuzzy controller for structures with hybrid isolation system. *Proc., 2nd World Conf. Structural Control*, Wiley, New York, TA2:67–76.
Nagarajaiah, S., Sahasrabudhe, S., and Iyer, R. (2000). 'Seismic response of sliding isolated bridges with MR dampers. *Proc., American Control Conference* (CD ROM)
Ogata, K. (1997). Modern control engineering. Prentice Hall, New Jersey.
Ramallo, J. C., Johnson, E. A., and Spencer, B. F., Jr. (2002). Smart base isolation systems. *Journal of Engineering Mechanics*, **128:10**, 1088–1099.
Reigles, D.G. and Symans, M.D. (2005). Systematic Performance Evaluation of Smart Seismic Isolation Systems. *Proc., Metropolis and Beyond - 2005 Structures Congress and 2005 Forensic Engineering Symposium*, New York, New York, U.S.A, American Society of Civil Engineers.
Reigles, D.G. and Symans, M.D. (2006). Supervisory fuzzy control of a base-isolated benchmark building utilizing a neuro-fuzzy model of controllable fluid viscous dampers. *Structural Control and Health Monitoring*, **13**, 724-747.
Skinner RI, Robinson WH, McVerry GH. (1993) An Introduction to Seismic Isolation. Wiley: Chichester, England.
Somerville, P., Smith, N., Punyamurthula, S., and Sun, J. (1997). Development of ground motion time histories for phase 2 of the FEMA/SAC steel project. *Report No. SAC/BD-97/04*, SAC Joint Venture, Sacramento, CA.
Spencer, B. F., Jr., and Sain, M. K. (1997). Controlling buildings: A new frontier in feedback. *IEEE Control Syst. Mag.*, **17:6**, 19–35.
Symans, M. D., and Kelly, S. W. (1999). Fuzzy logic control of bridge structures using intelligent semi-active seismic isolation systems. *Earthquake Engineering and Structural Dynamics*, **28**, 37–60.
Symans, M. D., Madden, G. J., and Wongprasert, N. (2000). Experimental study of an intelligent base isolation system for buildings. *Proc., 12th World Conf. on Earthquake Engineering*, Auckland, New Zealand.
Tsuchimoto et al. (2005). A Design of Advanced Base-Isolation System for Asymmetrical Building. *Proceedings, The 2005 World Sustainable Building Conference*, Tokyo, 27-29 September 2005, (SB05Tokyo)
Tu. J.Y., Lin, P.Y., Stoten, D.P. And Li, G. (2010). Testing of dynamically substructured, base-isolated systems using adaptive control techniques. *Earthquake Engineering and Structural Dynamics*, **39**, 661-681.
Wall, R.W. (2003) Simple methods for detecting zero crossing. *Proceedings of The 29th Annual Conference of the IEEE Industrial Electronics Society*, Paper # 000291.
Wongprasert, N. and Symans, M.D. (2005). Numerical Evaluation of Adaptive Base-Isolated Structures Subjected to Earthquake Ground Motions. *ASCE Journal of Engineering Mechanics*, **131:2**, 109-119.
Yoshioka H, Ramallo JC, Spencer Jr BF. (2002). Smart base isolation strategies employing magnetorheological dampers. *Journal of Engineering Mechanics* **128:5**, 540–551.
Zhang, Y. and Iwan, W.D.(2002) Protecting Base-Isolated Structures from Near-Field Ground Motion by Tuned Interaction Damper. *Journal of Engineering Mechanics*, **128:3**, 287-295.